

## PROCEEDINGS A

rspa.royalsocietypublishing.org



Article submitted to journal

**Subject Areas:**

Cosmology, Galaxies, Relativity

**Keywords:**Baryon Fraction, Galaxy Clusters,  
Theoretical Cosmology**Author for correspondence:**

F. Melia

e-mail: [fmelia@email.arizona.edu](mailto:fmelia@email.arizona.edu)

# Constancy of the Cluster Gas Mass Fraction in the $R_h = ct$ Universe

F. Melia

Department of Physics, The Applied Math Program,  
and Department of Astronomy, The University of  
Arizona, AZ 85721, USA

The ratio of baryonic to dark matter densities is assumed to have remained constant throughout the formation of structure. With this, simulations show that the fraction  $f_{\text{gas}}(z)$  of baryonic mass to total mass in galaxy clusters should be nearly constant with redshift  $z$ . However, the measurement of these quantities depends on the angular distance to the source, which evolves with  $z$  according to the assumed background cosmology. An accurate determination of  $f_{\text{gas}}(z)$  for a large sample of hot ( $kT_e > 5$  keV), dynamically relaxed clusters could therefore be used as a probe of the cosmological expansion up to  $z < 2$ . The fraction  $f_{\text{gas}}(z)$  would remain constant only when the “correct” cosmology is used to fit the data. In this paper, we compare the predicted gas mass fractions for both  $\Lambda$ CDM and the  $R_h = ct$  Universe and test them against the 3 largest cluster samples [1–3]. We show that  $R_h = ct$  is consistent with a constant  $f_{\text{gas}}$  in the redshift range  $z \lesssim 2$ , as was previously shown for the reference  $\Lambda$ CDM model (with parameter values  $H_0 = 70$  km s $^{-1}$  Mpc $^{-1}$ ,  $\Omega_m = 0.3$  and  $w_\Lambda = -1$ ). Unlike  $\Lambda$ CDM, however, the  $R_h = ct$  Universe has no free parameters to optimize in fitting the data. Model selection tools, such as the Akaike Information Criterion (AIC) and the Bayes Information Criterion (BIC), therefore tend to favor  $R_h = ct$  over  $\Lambda$ CDM. For example, the BIC favours  $R_h = ct$  with a likelihood of  $\sim 95\%$  versus  $\sim 5\%$  for  $\Lambda$ CDM.

## 1. Introduction

The idea that clusters might provide an independent probe of cosmological expansion took root following a series of non-radiative hydrodynamical simulations showing that the gas mass fraction,  $f_{\text{gas}} = M_{\text{gas}}/M_{\text{tot}}$ , in

the largest (i.e.,  $kT > 5$  keV) dynamically relaxed clusters, remains approximately constant with redshift [4,5]. Here,  $M_{\text{gas}}$  is the mass of the intracluster medium and  $M_{\text{tot}}$  is the total mass of the cluster. These results followed seminal papers by Sasaki [6] and Pen [7], who argued that the measurement of apparent evolution (or non-evolution) in  $f_{\text{gas}}$  could be used to examine the angular distance to these sources as a function of redshift. Since then, several groups have pursued this line of work, compiling extensive catalogs of clusters suitable for such a study [1–3,8,9]. In conjunction with this observational work, more elaborate simulations, incorporating several key physical ingredients, such as radiative cooling and the dynamical impact of turbulence, have provided a more realistic assessment of the conditions and cluster size for which  $f_{\text{gas}}$  might in fact be expected to remain constant.

Under the (as yet unproven) assumption that the baryonic to dark matter densities,  $\rho_b/\rho_d$ , is independent of redshift at least out to  $z \lesssim 2$ , the geometry of the Universe can be constrained in this way because the measured baryonic mass fraction depends on the assumed angular diameter distance to the source, which is used along with the inferred density to obtain  $M_{\text{gas}}$ . (This assumption may have to be modified if, and when, new physics beyond the standard model implies that baryons and/or dark matter may be created or annihilated with time since the big bang.) The baryonic matter content of galaxy clusters is dominated by the X-ray emitting intracluster gas, whose mass exceeds that of optically luminous material by a factor  $\sim 6$  [10,11]. The other contributions to the total baryon budget are expected to be very small. The emissivity of the X-ray emitting gas is proportional to the square of its density, so the gas mass profile in a cluster can be determined precisely from X-ray data. Measuring  $M_{\text{tot}}$  is more difficult because it is often based on the assumption of hydrostatic equilibrium in the gas, from which one may infer the depth of the gravitational potential required to maintain the density profile. Thus, only dynamically relaxed systems can be used for this purpose. In addition, as we will consider in more detail below, one would expect a constant mass fraction only for the very massive clusters, with minimal impact from astrophysical factors, such as feedback and cooling. But though cosmological simulations suggest that under some circumstances  $f_{\text{gas}}$  should be invariant with redshift, we would only see this in the data if the underlying model used to interpret the measurements is the correct cosmology. So in principle one may carry out a comparative test between competing models to see which, if any, predicts a constant value of  $f_{\text{gas}}$  with changing  $z$ .

### (a) The Constancy of $f_{\text{gas}}$

The caveat here is that the constancy of  $f_{\text{gas}}$  with redshift should be independent of the expansion dynamics. One would certainly be justified in expecting this if  $\rho_b/\rho_d$  has not changed with  $z$ . However, to use this feature as a cosmological tool, we have to believe that a sample of clusters exists for which  $f_{\text{gas}}$  is independent of which version of  $\Lambda$ CDM (or other cosmology) we are comparing with the data. For if the behavior of  $f_{\text{gas}}$  with redshift were different for different expansion rates, we could not be certain that  $f_{\text{gas}}$  should in fact remain constant.

In their high-resolution simulations, Kravtsov et al. [12] incorporated the effects of radiative cooling and galaxy formation on the baryon fraction, including the impact on star formation, metal enrichment, and stellar feedback. These processes increase the total baryon fraction within scales as large as the virial radius, though it is within the cluster cores that baryon fractions larger than the universal value are seen. However, even with cooling, the cumulative baryon fraction is close to its universal value at radii  $r > r_{2,500}$ , where  $r_{\Delta}$  is defined to be the radius within which the average cluster density is greater than its critical value by a factor  $\Delta$  at that redshift (see equation 2.12 below). Moreover, even though the baryon fraction may be different from its universal value at smaller radii, simulations such as this suggest that the total baryon fraction within the cluster virial radius does not evolve with time, regardless of whether or not cooling is included.

Simulations with even greater sophistication than these were carried out by Ettori et al. [13], this time including also the effects of feedback through galactic winds and conduction. They found that the baryon fraction within a fixed overdensity increases slightly with redshift, though the impact at large cluster-centric distances (i.e.,  $r > r_{500}$ ) is nearly independent of the physics included in the calculations. More recently, Planelles et al. [14] updated these simulations by including feedback from supernovae and active galactic nuclei. They too found that the baryon fraction is nearly independent of the physical processes, and is characterized by a negligible redshift evolution, if the cluster mass  $M_{500}$  at  $r_{500}$  is  $\gtrsim 10^{14} M_{\odot}$ . At smaller radii,  $r_{2,500}$ , its value slightly decreases, while its scatter increases by about a factor of 2. As we shall see, the cluster catalogs currently available for this cosmological test differ in their assumed overdensity factor  $\Delta$ , so  $f_{\text{gas}}$  may not be uniformly constant with redshift from sample to sample. This is an important caveat to consider when weighing the results of model comparisons using different cluster catalogs. In this paper, we will consider the 3 largest samples, two of which assume  $\Delta = 2,500$  [1,2], while the third adopts the value  $\Delta = 500$  [3].

### (b) Testing Cosmological Models with $f_{\text{gas}}$

Up until now, the cluster gas mass fraction has been used to probe only the parameter space associated with the standard model of cosmology,  $\Lambda$ CDM. The reference model often used for this work assumes a spatially flat universe ( $k=0$ ) with a scaled matter density  $\Omega_m \equiv \rho_m/\rho_c = 0.3$ , where  $\rho_m = \rho_b + \rho_d$  is the matter density and  $\rho_c \equiv 3c^2 H_0^2/8\pi G$  is the critical density in terms of the Hubble constant  $H_0$  today, and a dark energy in the form of a cosmological constant with equation-of-state  $w_{\Lambda} \equiv p_{\Lambda}/\rho_{\Lambda} = -1$ , in terms of its pressure  $p_{\Lambda}$  and density  $\rho_{\Lambda}$ . Since these clusters lie at redshifts  $z < 1.5$ , where the contribution of radiation to the total energy density is below detectability, one can also assume that  $\Omega_m + \Omega_{\Lambda} = 1$ . In obvious notation,  $\Omega_{\Lambda} \equiv \rho_{\Lambda}/\rho_c$ .

But in recent years, evidence has been accumulating that  $\Lambda$ CDM is perhaps the empirical approximation to a more theoretically motivated FRW cosmology known as the  $R_h = ct$  Universe [15–17]. (A somewhat pedagogical treatment may be found in ref. [18].) The latter arises when one invokes Birkhoff's theorem [19] together with Weyl's postulate [20], which lead to an identification of the Hubble radius  $R_h = c/H$  as another manifestation of the Universe's gravitational horizon,  $2GM/c^2$ , defined in terms of the Misner-Sharp mass  $M$  contained within a proper spherical volume of radius  $R_h$  [21]. It must therefore itself be a proper distance  $R_h = a(t)r_h$ , where  $a(t)$  is the universal expansion factor and  $r_h$  is an unchanging co-moving distance. This form of  $R_h$  leads immediately to the condition that  $\dot{a} = \text{constant}$ . Thus, the  $R_h = ct$  Universe expands at a constant rate.

This cosmology should not be confused with the Milne Universe [22], which is empty and has negative spatial curvature ( $k = -1$ ). The Milne Universe does not at all fit the cosmological data and was ruled out as a viable model long ago. Instead, the  $R_h = ct$  Universe is flat ( $k = 0$ ) and predicts very simple, analytical forms for measurable quantities, such as the luminosity distance,

$$d_L^{R_h} = R_h(1+z) \ln(1+z), \quad (1.1)$$

and the redshift dependence of the Hubble constant,

$$H(z) = H_0(1+z). \quad (1.2)$$

We will provide a more detailed description of the differences between  $R_h = ct$  and  $\Lambda$ CDM in § 3 below.

By now, the predictions of these two cosmologies have been compared to each other using many diverse tests and available data, including: the cosmic chronometers [23], the gamma-ray burst Hubble diagram [24], the high- $z$  quasars [25], the angular correlation function of the cosmic microwave background radiation [26], and the high- $z$  galaxies [27], among others (some not yet published). The consensus from all of this work appears to be that the  $R_h = ct$  Universe is closer to the correct cosmology than  $\Lambda$ CDM is.

In this paper, we extend this comparative study even further, by now examining the role played by the  $R_{\text{h}} = ct$  Universe in maintaining an approximately constant value of the cluster gas mass fraction in the redshift range  $z \lesssim 2$ . In §2 of this paper, we briefly describe the basic theory behind this independent cosmological probe. In §3, we discuss the assumptions necessary in both  $\Lambda$ CDM and  $R_{\text{h}} = ct$  to make this diagnostic meaningful for cosmology, and then assemble the most extensive catalogs now available in §4. We carry out our direct comparison between  $\Lambda$ CDM and  $R_{\text{h}} = ct$  in §5, and then discuss our results and place them in a proper context in §6.

## 2. The Use of Cluster Gas Mass Fraction as a Cosmological Probe

The baryonic matter content of galaxy clusters is dominated by the X-ray-emitting intracluster gas predominantly via thermal bremsstrahlung [28]. Thus, for the spherical  $\beta$ -model profile [29], the gas mass  $M_{\text{gas}}(< R)$  within a radius  $R$  derived from X-ray observations may be written

$$M_{\text{gas}}(< R) = \left[ \frac{3\pi\hbar m_e c^2}{2(1+X)e^6} \right]^{1/2} \left( \frac{3m_e c^2}{2\pi k_B T_e} \right)^{1/4} m_H \times \frac{1}{[\bar{g}_B(T_e)]^{1/2}} r_c^{3/2} \left[ \frac{I_M(R/r_c, \beta)}{I_L^{1/2}(R/r_c, \beta)} \right] [L_X(< R)]^{1/2}, \quad (2.1)$$

where  $m_e$  and  $m_H$  are the electron and hydrogen masses, respectively,  $X$  is the hydrogen fraction by mass,  $T_e$  is the (electron) gas temperature,  $\bar{g}_B(T_e)$  is the Gaunt factor,  $r_c$  is the core radius, and  $I_M(y, \beta) \equiv \int_0^y (1+u^2)^{-3\beta/2} u^2 du$ ,  $I_L(y, \beta) \equiv \int_0^y (1+u^2)^{-3\beta} u^2 du$ . The chosen cosmology enters this expression in three ways: through the X-ray luminosity

$$L_X(< R) = 4\pi d_L^2 f_X(< \theta), \quad (2.2)$$

through the core radius

$$r_c = \theta_c d_A, \quad (2.3)$$

and through the variable radius

$$R = \theta d_A, \quad (2.4)$$

in terms of the observed angular size  $\theta$ , the observed X-ray flux  $f_X$ , and the luminosity ( $d_L$ ) and angular ( $d_A$ ) distances. Some of the data we will examine below are based on observations of the Sunyaev-Zeldovich effect (SZE), for which  $M_{\text{gas}}$  depends on a different power of radius. For the SZE objects,  $M_{\text{gas}} \propto d_A^2$ , instead of  $\propto d_L d_A^{3/2}$  [1], which is applicable in all other cases:

$$M_{\text{gas}}(z, < \theta) \propto d_L d_A^{3/2}. \quad (2.5)$$

And since  $d_A = (1+z)^{-2} d_L$ , we have

$$M_{\text{gas}}(z, < \theta) \propto d_A^{5/2} \quad (2.6)$$

at any given redshift  $z$ .

Under the assumption of hydrostatic equilibrium and isothermality ( $T_e = \text{constant}$ ), the total mass within radius  $R$  is given by

$$M_{\text{tot}}(< R) = - \frac{k_B T_e R}{G\mu m_H} \left. \frac{d \ln n_e(r)}{d \ln r} \right|_{r=R}, \quad (2.7)$$

where  $\mu$  is the mean-molecular weight per particle and  $n_e(r)$  is the spatially-dependent electron number density. Thus, one gets

$$M_{\text{tot}}(< \theta) \propto d_A, \quad (2.8)$$

and therefore

$$f_{\text{gas}} \propto d_A^{3/2}. \quad (2.9)$$

According to Equation (1.1), the angular distance in these expressions takes on a very simple analytical form in the  $R_h = ct$  Universe:

$$d_A^{R_h} = \frac{R_h}{(1+z)} \ln(1+z). \quad (2.10)$$

The corresponding expression in  $\Lambda$ CDM is

$$d_A^{\Lambda} = \frac{R_h}{(1+z)} \frac{1}{\sqrt{|\Omega_k|}} \operatorname{sinn} \left\{ |\Omega_k|^{1/2} \times \int_0^z \frac{dz}{\sqrt{(1+z)^2(1+\Omega_m z) - z(2+z)\Omega_\Lambda}} \right\}. \quad (2.11)$$

In this equation,  $\Omega_k$  represents the spatial curvature of the Universe—appearing as a term proportional to the spatial curvature constant  $k$  in the Friedmann equation. In addition,  $\operatorname{sinn}$  is  $\sinh$  when  $\Omega_k > 0$  and  $\sin$  when  $\Omega_k < 0$ . For a flat Universe with  $\Omega_k = 0$ , which is what we assume throughout this paper, this equation simplifies to the form  $R_h/(1+z)$  times the integral. The conversion from one cosmology to another therefore reduces predominantly to an evaluation of Equations (2.10) and (2.11).

But before we move on to the cluster samples, and carry out this comparison, there is an additional ingredient one must incorporate into the calculation of  $f_{\text{gas}}$ , and this has to do with the measurement radius used to delimit the volume over which  $M_{\text{gas}}$  and  $M_{\text{tot}}$  are determined. This radius is selected by fixing the value of cluster overdensity,

$$\Delta \equiv \frac{3M_{\text{tot}}(< R_\Delta)}{4\pi\rho_c(z_{\text{cluster}})r_\Delta^3}, \quad (2.12)$$

at its inferred redshift  $z_{\text{cluster}}$ . Often,  $\Delta$  is taken to be 2,500 (as in refs. [1,2]; see next section), but not always. (This is one of several reasons why we cannot combine all of the available samples to carry out a single fitting procedure. As we shall see in the next section, it is necessary to carry out the fitting for each individual compilation of sources. Some discussion concerning which value is more trustworthy in measuring  $f_{\text{gas}}$  appears in refs. [30,31].) The third data set we are using [3] assumes  $\Delta = 500$ .

So there is an additional dependence of  $f_{\text{gas}}$  on the background cosmology, beyond simply the factor appearing in Equation (2.9), because  $r_{2,500}$  (or  $r_{500}$ ) itself changes with the model. The reasoning behind this is rather simple to understand [2]. On the one hand, we know that the total mass within  $r_{2,500}$  is given by the expression  $M_{2,500} = (4\pi/3)r_{2,500}^3(2,500\rho_c)$ . But since both  $T_e$  and the density gradient in Equation (2.7) are approximately constant in the region of  $\theta_{2,500}$ , the hydrostatic equilibrium equation gives  $M_{2,500} \propto r_{2,500}$  (see Equation 2.8). These two expressions should be equal, and since  $\rho_c \sim H(z)^2$ , we see that  $r_{2,500} \sim H(z)^{-1}$ . Thus, the angle spanned by  $r_{2,500}$  at  $z$  is  $\theta_{2,500} = r_{2,500}/d_A \sim (H d_A)^{-1}$ . According to ref. [2], the slope of  $f_{\text{gas}}(r/r_{2,500})$  in the region of  $r_{2,500}$  is  $\eta \sim 0.214 \pm 0.022$  over their sample range  $0.7 < r/r_{2,500} < 1.2$ , for the reference  $\Lambda$ CDM model described in the introduction. Therefore, since the angle subtended by  $r_{2,500}$  changes with the cosmology, one expects that  $f_{\text{gas}} \sim \theta_{2,500}^{-\eta} \sim (H d_A)^\eta$ , over and above the primary dependence given in Equation (2.9). This angular correction factor is close to unity for all cosmologies and redshifts of interest, but ought to be included for completeness.

Given the strong dependence of the inferred values of  $M_{\text{gas}}$  and  $M_{\text{tot}}$  on the assumed cosmology, the data need to be recalibrated for each considered model. However, a procedure has been developed by the groups who analyze these clusters, in which the data are reduced once for the reference  $\Lambda$ CDM model, and then are fitted with modifications to the reference model based on its differences with the cosmology being tested. Specifically, the model fitted to the reference  $\Lambda$ CDM data takes the form

$$f_{\text{gas}}^{\text{model}} = K \left[ \frac{H(z) d_A(z)}{[H(z) d_A(z)]^{\Lambda\text{CDM}}} \right]^\eta \left[ \frac{d_A^{\Lambda\text{CDM}}(z)}{d_A(z)} \right]^{3/2}, \quad (2.13)$$

where  $K$  is a constant that includes a parametrization of the residual uncertainty in the accuracy of the instrument calibration and X-ray modelling, and the factors in brackets represent the two

principal dependencies described above, i.e., on  $d_A^{3/2}$  and  $\theta_{2,500}^\eta$ . In this expression, the variables with superscript  $\Lambda$ CDM have values corresponding to the reference  $\Lambda$ CDM model (see §1 above), whereas the unlabeled parameters are those representing the new cosmological model being tested (in this case,  $R_h = ct$ ). Sometimes, additional factors are added to this expression, e.g., representing the possible contribution from nonthermal pressure support, the  $z$  dependence of the baryonic mass fraction in stars, and a possible evolutionary depletion of the baryon fraction measured at  $r_{2,500}$  as a consequence of the thermodynamic history of the gas [2]. All these factors, however, appear to be very close to unity, and we will therefore not include them in our analysis.

### 3. Theoretical Background

The appropriate spacetime to use in any cosmological model is conveniently and elegantly written in terms of the Friedmann–Robertson–Walker (FRW) metric, though this does not tell us much about the cosmic equation of state (EOS), relating the total energy density  $\rho$  to its total pressure  $p$ . If the EOS were known, the dynamical equations governing the Universal expansion could be solved exactly, and the observations could then be interpreted unambiguously. Unfortunately, we must rely on measurements and assumptions to pick  $\rho$  and  $p$ . At the very minimum,  $\rho$  must contain matter  $\rho_m$  and radiation  $\rho_r$ , which we see directly, and an as yet poorly understood ‘dark’ energy  $\rho_{de}$ , whose presence is required by a broad range of data including the Type Ia supernova Hubble diagram [32,33].

However, as the measurements of the distance versus redshift continue to improve, they appear to be creating more tension between theory and observations, rather than providing us with a better indication of the dark-energy component,  $p_{de} = w_{de}\rho_{de}$ . For example, this is seen with the difficulty  $\Lambda$ CDM has in accounting for the growth and evolution of high- $z$  quasars [25] and high- $z$  galaxies [27]. It is also apparent from the  $2.5\sigma$  disparity between the predictions of  $\Lambda$ CDM and the precise measurements using the Alcock–Paczynski test ( $\mathcal{D}(z) = d_A(z)H(z)/c$ ) applied to galaxy clusters [34]. Of the 3 measurements made to date,  $\mathcal{D}(0.35) = 0.286 \pm 0.025$ ,  $\mathcal{D}(0.57) = 0.436 \pm 0.052$ , and  $\mathcal{D}(2.34) = 1.229 \pm 0.110$ ,  $\Lambda$ CDM predicts  $\mathcal{D}^{\Lambda\text{CDM}}(0.35) = 0.325$ ,  $\mathcal{D}^{\Lambda\text{CDM}}(0.57) = 0.500$ , and  $\mathcal{D}^{\Lambda\text{CDM}}(2.34) = 1.354$ . By contrast,  $R_h = ct$  provides a much better accounting of these data, with  $\mathcal{D}^{R_h=ct}(0.35) = 0.300$ ,  $\mathcal{D}^{R_h=ct}(0.57) = 0.451$  and  $\mathcal{D}^{R_h=ct}(2.34) = 1.206$ . And as a third example, the best-fit value of  $H_0 = 67.3 \pm 1.2 \text{ km s}^{-1} \text{ Mpc}^{-1}$  measured by *Planck* [35] is quite different from that ( $\sim 70 - 72 \text{ km s}^{-1} \text{ Mpc}^{-1}$ ) inferred from low-redshift measurements, e.g., using the Type Ia SN Hubble diagram.

$\Lambda$ CDM assumes that dark energy is a cosmological constant  $\Lambda$  with  $w_{de} \equiv w_\Lambda = -1$ , and therefore  $w = (\rho_r/3 - \rho_\Lambda)/\rho$ . This model does quite well explaining many of the observations, but such a scenario is inadequate to explain all of the nuances seen in cosmic evolution and the growth of structure. For example, insofar as the CMB fluctuations measured with both WMAP [36] and *Planck* [35] are concerned, there appears to be unresolvable tension between the predicted and measured angular correlation function [26,37–39]. Also, the observed galaxy distribution function appears to be scale-free, whereas the matter distribution expected in  $\Lambda$ CDM has a different form on different spatial scales. The fine tuning required to resolve this difference led Watson et al. [40] to characterize the galactic matter distribution function as a ‘cosmic coincidence.’ (We note, however, that the galaxy correlation function may be a poor indicator of the matter distribution itself, since the former depends on the still uncertain nature of galaxy formation, in addition to the underlying cosmology.) Such difficulties are compounded by  $\Lambda$ CDM’s predicted redshift-age relation, which does not appear to be consistent with the growth of quasars at high redshift [25], nor the very early appearance of galaxies at  $z \gtrsim 10$  [27].

The  $R_h = ct$  Universe is another FRW cosmology that has much in common with  $\Lambda$ CDM, but includes an additional ingredient motivated by several theoretical and observational arguments [15–17]. Like  $\Lambda$ CDM, it also adopts the equation of state  $p = w\rho$ , with  $p = p_m + p_r + p_{de}$  and  $\rho = \rho_m + \rho_r + \rho_{de}$ , but goes one step further by specifying that  $w = (\rho_r/3 + w_{de}\rho_{de})/\rho = -1/3$  at all times. One might come away with the impression that these two prescriptions for the equation of

state cannot be consistent. But in fact nature is telling us that if we ignore the constraint  $w = -1/3$  and instead proceed to optimize the parameters in  $\Lambda$ CDM by fitting the data, the resultant value of  $w$  averaged over a Hubble time is actually  $-1/3$  within the measurement errors [15,17]. In other words, though  $w = (\rho_r/3 - \rho_\Lambda)/\rho$  in  $\Lambda$ CDM cannot be equal to  $-1/3$  from one moment to the next, its value averaged over the age of the Universe is equal to what it would have been in  $R_h = ct$ .

This result does not necessarily prove that  $\Lambda$ CDM is an incomplete version of  $R_h = ct$ , but it does seem to suggest that the inclusion of the additional constraint  $w = -1/3$  might render its predictions closer to the data. In  $R_h = ct$ , this condition on the total equation of state is required in order to maintain a constant expansion rate  $a(t) \propto t$ . Thus, the principal difference between  $\Lambda$ CDM and  $R_h = ct$  is that, whereas one must first assume the constituents and their equations of state in  $\Lambda$ CDM and then infer its expansion rate, the Universe's dynamics in  $R_h = ct$  is completely specified before one begins to speculate on its contents.

Nonetheless, both  $\Lambda$ CDM and  $R_h = ct$  face similar limitations when it comes to the essential ingredients in the cosmic fluid, such as the nature of dark matter or dark energy. In  $\Lambda$ CDM, one of the most important assumptions is that  $\rho_b/\rho_d$  is constant with redshift (and therefore time). Of course, the distribution of halos, and eventually galaxies and clusters, depends on the background expansion rate (for a recent set of simulations, see ref. [14]). However, the many calculations carried out to date suggest that the gas mass fraction in clusters is insensitive to the underlying cosmology.

There is actually a good, sound reason for the relative insensitivity of the structure and content of a condensing halo to the choice of underlying cosmology. One may understand this basic outcome in the context of Birkhoff's theorem and its corollary [15,19], according to which the spacetime inside of a spherical shell in an otherwise isotropic distribution of mass and energy is completely independent of the exterior region. Because of spherical symmetry, all contributions to the spacetime curvature within this shell cancel completely. Thus, once an overdense perturbation in the background density begins to be self-gravitating and forms a bound system, its subsequent evolution proceeds under its own gravity, independently of the surrounding medium, even in an infinite universe. The expansion rate exterior to the contracting halo therefore has little influence on the eventual structure and content of the collapsing region. All the simulations confirm this basic result—actually going even farther and showing that the inclusion of additional astrophysical effects, such as radiative cooling, have only a minimal impact on the results.

In other words, because of Birkhoff's theorem, if  $f_{\text{gas}}$  is more or less constant in any one model, it is expected to be similarly constant in all cosmological models, but we would measure it to be independent of redshift only if the correct geometry were assumed in the data analysis. This is what makes it such a potentially powerful probe of the cosmology. Insofar as the  $R_h = ct$  Universe is concerned, detailed hydrodynamical simulations of structure formation do not yet exist. But because of Birkhoff's theorem and the insensitivity of the halo evolution to the external expansion rate, we can already start to examine the possibility that  $f_{\text{gas}}$  may be constant in this cosmology as well, with more in-depth analysis to follow after comprehensive structure formation simulations will have been completed.

Nonetheless, to make a model comparison viable, we need to consider several essential constraints. At the very minimum, the  $R_h = ct$  Universe must also contain baryonic matter, radiation, dark matter, and some form of dark energy, though we already know that this could not be a cosmological constant. What we do know, however, is that no matter what these ingredients turn out to be, they must always partition themselves in such a way as to maintain the total equation of state  $p = -\rho/3$ . The idea that the internal chemistry of a system adjusts to macroscopic constraints is not uncommon. For example, we already have such a situation with  $\Lambda$ CDM, where the partitioning of baryonic matter and radiation in the early universe follows the prescribed redshift evolution in temperature  $T(z)$ . Moreover, since the existence of dark matter and dark energy presumably implies physics beyond the standard model, it's quite possible that this early partitioning of the constituents in  $\Lambda$ CDM involves other components, in addition to baryonic matter and radiation.

Recently, the validity of the  $R_h = ct$  model was questioned on the basis that its equation of state could not be consistent with the conservation of matter during the Universe's expansion [42]. This argument took the opposite approach to what we have just described, i.e., it abandoned the equation of state  $p = -\rho/3$  and instead replaced it with a  $\Lambda$ CDM-like sum of the equations of state of individual constituents, but with the added proviso that matter could not be created or annihilated once it appeared on the scene. This begs the question of how matter could have been created in the first place, not to mention how such an unmotivated constraint could be consistent with what we believe happened with  $\Lambda$ CDM in the early Universe, when matter and radiation (and possibly other as yet unknown fields) transformed back and forth into each other prior to, and subsequent to, the period of inflation. It's always interesting to explore the viability of such variants to the basic model, but one should not interpret their results as being meaningful to the  $R_h = ct$  Universe, which does not incorporate the conservation of matter as one of its basic ingredients. The only condition essential to this cosmology is the total equation of state  $p = -\rho/3$ , which no doubt will impact how we interpret physics beyond the standard model.

In our recent analysis of the Epoch of Reionization [41], we considered the possibility that the dark matter and baryonic densities might have evolved separately of each other at high redshifts, i.e.,  $6 \lesssim z \lesssim 15$ . However, it is not clear whether such a trend might continue to lower redshifts. There is clearly much to learn from future developments in particle physics, for both  $\Lambda$ CDM and  $R_h = ct$ . But insofar as understanding the redshift dependence of the gas mass fraction  $f_{\text{gas}}$  is concerned, we will here make the simplest minimal assumption for both  $R_h = ct$  and  $\Lambda$ CDM, which is that the baryonic fraction  $\rho_b/\rho_d$  remains approximately constant for  $z \lesssim 2$ . The results of this paper are contingent upon the validity of this assumption.

## 4. The Principal Data Sets

In order to compare the predictions of the  $R_h = ct$  Universe against those of the reference  $\Lambda$ CDM model, we consider three samples of galaxy clusters whose gas mass fractions have been measured using X-ray surface brightness observations. The LaRoque et al. sample [1] consists of 38 massive clusters lying in the redshift range  $0.14 < z < 0.89$ , and were obtained from *Chandra* X-ray and OVRO/BIMA interferometric Sunyaev-Zeldovich Effect measurements. In order to study the dependence of their analysis on the assumed model for the cluster gas distribution, taking into account the possible presence of a cooling flow, these authors considered three different models for the plasma profile: (1) an isothermal  $\beta$ -model fit jointly to the X-ray data at radii beyond 100 kpc and to all of the SZE data, (2) a nonisothermal double  $\beta$ -model in hydrostatic equilibrium, fit jointly to all of the X-ray and SZE data, and (3) an isothermal  $\beta$ -model fit only to the SZE spatial data. In this paper, we consider the results of models (1) and (2) only, since the number of clusters appropriate for the third case was noticeably smaller than the others. The single isothermal  $\beta$ -model with the central 100 kpc excised seemed to work quite well, since the cut was large enough to exclude the cooling region in cool-core clusters while keeping a sufficient number of photons to enable the mass modelling. The more sophisticated double- $\beta$  model was designed to take into account (non-isothermal) temperature profiles, and was developed to assess the biases arising from the isothermal assumption and the effects of core exclusion in the first model. As we will see in the next section, the fits suggest that both of these approaches work quite well, and provide mutually consistent results.

Our second sample is taken from Allen et al. [2], who compiled a catalog of 42 hot ( $kT_e > 5$  keV), X-ray luminous, dynamically relaxed galaxy clusters spanning the redshift range  $0.05 < z < 1.1$ . Their measurements were also based on *Chandra* observations, and like ref. [1], these authors also adopted a canonical measurement radius of  $r_{2,500}$ , whose value they determined directly from the *Chandra* data. Ten of these clusters are in common with a subset of the LaRoque sample, and there is good agreement for the best-fitting results in this sub-sample at  $r_{2,500}$  between the two groups, though the mass fractions measured by LaRoque et al. are on average about 6 percent higher than those reported in ref. [1] for the systems in common.

The Ettori et al. [3] sample is the biggest of the three, containing 52 X-ray luminous galaxy clusters (also observed with *Chandra*) in the redshift range  $0.3 < z < 1.273$ , merged with 8 additional objects at  $0.06 < z < 0.23$ , with a gas temperature  $> 4$  keV [30]. Note, however, that although the reference cosmology (as described in §1 above) is identical for all three samples, ref. [3] decided to use an overdensity of 500 (instead of 2,500) to define the outer radius of their mass determination region. Strictly speaking, this means that  $\eta$  (see Equation 2.13) could be different from the value ( $\sim 0.2$ ) applied to the other two samples, but for the sake of simplicity, we will use the same value throughout our analysis. Since this index is presumably much smaller than one, the impact of this approximation on our results is expected to be smaller than, e.g., the errors on the sample means of the  $f_{\text{gas}}$  values. Another technical difference among the samples is that both the Allen et al. [2] and Ettori et al. [3] measurements of the mass fraction  $f_{\text{gas}}$  are based strictly on the assumption of isothermality and hydrostatic equilibrium, in contrast to ref. [1], which considered both isothermal and nonisothermal models. Such differences in the handling of the various samples precludes any possibility of merging them into a single, bigger sample, thereby improving the statistics. On the other hand, the fact that the approaches were somewhat different lends some credence to the results when they agree with each other within the errors.

## 5. A Direct Comparison between $\Lambda$ CDM and $R_{\text{h}} = ct$

Non-radiative simulations of large clusters suggest that  $f_{\text{gas}}$  should be approximately constant with redshift [4,5,14], at least for  $z \lesssim 2$ . Let us now compare the measured values of  $f_{\text{gas}}$ , based on the reference  $\Lambda$ CDM model, with those re-calibrated for the  $R_{\text{h}} = ct$  Universe using Equation (2.13). For each sample, we calculate the  $\chi^2$  function,

$$\chi^2 = \sum_{i=1}^N \frac{(f_{\text{gas},i} - f_{\text{gas}})^2}{\sigma_i^2 + \sigma_f^2}, \quad (5.1)$$

where  $N$  is the sample size,  $f_{\text{gas},i}$  and  $\sigma_i$  are the single gas mass fraction measurements and their relative errors,  $f_{\text{gas}}$  is the constant gas fraction to be optimized while finding the best fit to the  $f_{\text{gas},i}$  values, and  $\sigma_f$  is its error, calculated from the population standard deviation [3].

The Hubble constant itself does not affect the comparison between the two models. Therefore, fits to the data using the  $R_{\text{h}} = ct$  Universe have no free parameters. One can see this directly from Equation (2.10), in which the removal of  $R_{\text{h}}$ , i.e., the Hubble constant, leaves no flexibility at all for the angular distance as a function of redshift.  $\Lambda$ CDM, on the other hand, has anywhere from 2 to 6 free parameters, in addition to  $H_0$ , depending on how one chooses to treat the dark energy and its equation of state. Here, we conservatively take the minimum number, i.e., 2, these being the value of  $\Omega_m$  and  $w_\Lambda$ , the two parameters (besides  $H_0$ ) used to calculate  $f_{\text{gas}}$  in the three samples.

To facilitate a quick visual comparison between the various models, we show in figures 1-3 the data obtained for the reference  $\Lambda$ CDM cosmology, paired with the same set of data re-calibrated for the  $R_{\text{h}} = ct$  Universe. As described above, this re-calibration is not necessary to produce the fits and their  $\chi^2$  values, and is carried out solely for the purpose of yielding an immediate visual impact of the differences between the two.

In all three samples, both cosmologies are consistent with the expectation of a constant  $f_{\text{gas}}$ , though slight differences emerge for the values of  $f_{\text{gas}}$  and  $\chi_{\text{dof}}^2$ . However, the fact that the number of free parameters is different between these models leads to significantly different likelihoods of either being closer to the correct cosmology, as we shall describe in the next section. But for now, starting with the most recently measured sample [3], we find that the reference  $\Lambda$ CDM model yields  $f_{\text{gas}} = 0.114 \pm 0.041$ , with  $\chi_{\text{dof}}^2 = 0.57$ , for  $60 - 2 = 58$  degrees of freedom. By comparison, the fit using  $R_{\text{h}} = ct$  results in  $f_{\text{gas}} = 0.117 \pm 0.043$ , with  $\chi_{\text{dof}}^2 = 0.56$ , for 60 degrees of freedom. The fits are comparable, though with very slight differences in the average gas mass fraction (see figure 1).

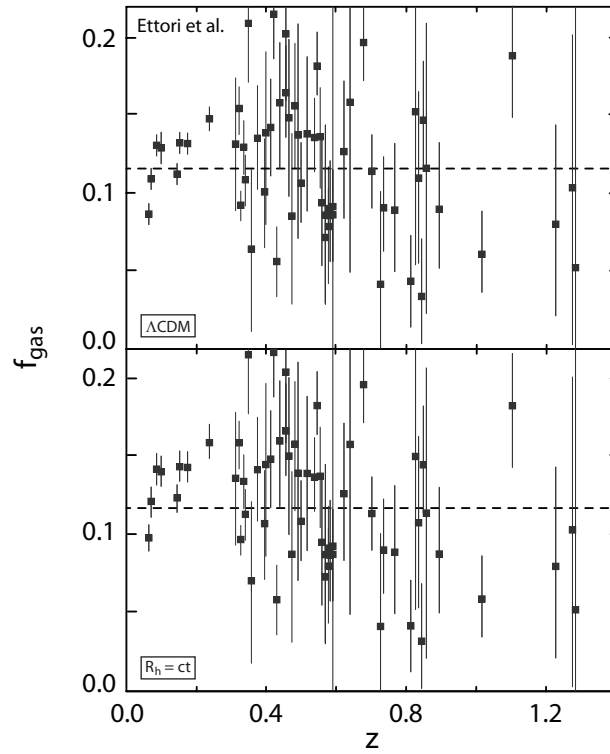


**Figure 1.** The apparent variation of the X-ray gas mass fraction measured within  $r_{500}$  as a function of redshift for the 60 clusters in Ettori et al. (2009). In the upper panel are the values for the reference  $\Lambda$ CDM model ( $\Omega_m = 0.3$ ,  $h \equiv H_0/100 \text{ km s}^{-1} \text{ Mpc}^{-1} = 0.7$ , and  $w_{\text{de}} = -1$ ). In the lower panel, are the values for the  $R_h = ct$  Universe, using the same Hubble constant  $h$ . Both results are consistent with the expectation of a constant  $f_{\text{gas}}(z)$  (dashed lines) from simulations. The reference  $\Lambda$ CDM fit yields  $f_{\text{gas}} = 0.114 \pm 0.041$ , with  $\chi_{\text{dof}}^2 = 0.57$  for 58 degrees of freedom, while fitting with the  $R_h = ct$  Universe yields  $f_{\text{gas}} = 0.117 \pm 0.043$ , with  $\chi_{\text{dof}}^2 = 0.56$  for 60 degrees of freedom. By comparison, the cosmic ratio  $\rho_b/(\rho_b + \rho_d)$  measured by *Planck* is  $0.155 \pm 0.006$  [35], and  $0.166 \pm 0.013$  measured by WMAP-9 [39].

For the Allen et al. [2] sample (figure 2), we find using this approach that the reference  $\Lambda$ CDM model yields  $f_{\text{gas}} = 0.110 \pm 0.016$  with  $\chi_{\text{dof}}^2 = 0.42$  for  $42 - 2 = 40$  degrees of freedom, while fitting with  $R_h = ct$  gives  $f_{\text{gas}} = 0.116 \pm 0.017$  and  $\chi_{\text{dof}}^2 = 0.45$  for 42 degrees of freedom.

In the LaRoque et al. [1] sample, we consider the isothermal (with a 100-kpc cut) cases (figures 3.a and 3.c) separately from the non-isothermal cases (figures 3.b and 3.d), and also the X-ray observed gas mass fractions (figures 3.a and 3.b) separately from those obtained via measurements of the SZE (figures 3.c and 3.d). In these figures, the data include both cool-core (triangles) and non-cool-core subsamples (squares). This sample includes a subgroup of clusters with bright and sharply peaked cores; they are referred to as cool-core clusters because the sharply peaked X-ray emission is indicative of strong radiative cooling in cluster core. The individual values of  $f_{\text{gas}}$  and  $\chi_{\text{dof}}^2$  are quoted in the figure captions, and range over  $f_{\text{gas}} \sim 0.108 \pm 0.020$  to  $0.120 \pm 0.032$  with  $\chi_{\text{dof}}^2 \sim 0.59 - 0.88$  for the reference  $\Lambda$ CDM model, and  $f_{\text{gas}} \sim 0.114 \pm 0.021$  to  $0.124 \pm 0.022$  with  $\chi_{\text{dof}}^2 \sim 0.57 - 0.86$  for the  $R_h = ct$  Universe.

## 6. Discussion and Conclusions

The results presented in the previous section demonstrate that both the reference  $\Lambda$ CDM cosmology and the  $R_h = ct$  Universe are consistent with a constant value of the cluster gas mass

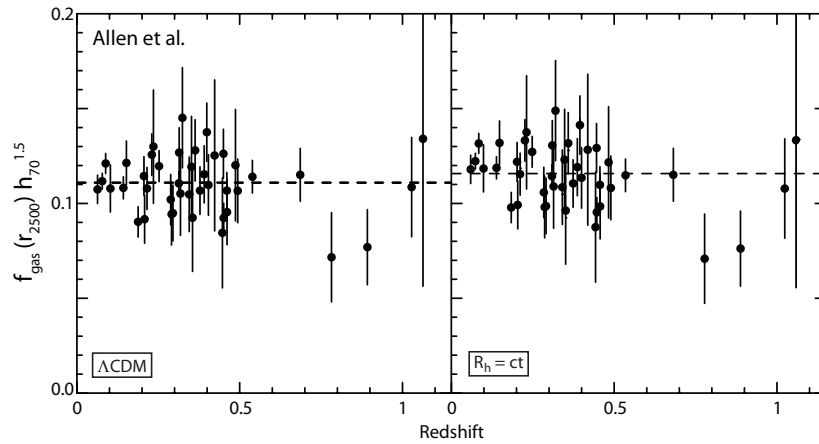


**Figure 2.** The apparent variation of the X-ray gas mass fraction measured within  $r_{2500}$  as a function of redshift for the 42 clusters in Allen et al. [2]. On the left are the values for the reference  $\Lambda$ CDM model ( $\Omega_m = 0.3$ ,  $h \equiv H_0/100 \text{ km s}^{-1} \text{ Mpc}^{-1} = 0.7$ , and  $w_{de} = -1$ ). On the right, are the values for the  $R_h = ct$  Universe, using the same Hubble constant  $h$  (though  $h$  has no effect on this plot). Both results are consistent with the expectation of a constant  $f_{\text{gas}}(z)$  (dashed lines) from simulations. The reference  $\Lambda$ CDM fit yields  $f_{\text{gas}} = 0.110 \pm 0.016$ , with  $\chi^2_{\text{dof}} = 0.42$  for 40 degrees of freedom, while fitting with the  $R_h = ct$  Universe yields  $f_{\text{gas}} = 0.116 \pm 0.017$ , with  $\chi^2_{\text{dof}} = 0.45$  for 42 degrees of freedom. By comparison, the cosmic ratio  $\rho_b/(\rho_b + \rho_d)$  measured by *Planck* is  $0.155 \pm 0.006$  [35], and  $0.166 \pm 0.013$  measured by WMAP-9 [39].

fraction with increasing redshift, under the underlying assumption that the baryonic fraction  $\rho_b/\rho_d$  has remained constant during the most significant period of structure formation (i.e.,  $z \lesssim 3-4$ ).

The fact that the  $R_h = ct$  Universe fits these data so well is probably the reason why some previous work with clusters had already hinted at a possible deviation from accelerated expansion, even though  $R_h = ct$  was not known or used in those studies [43]. Using the 42 measurements from ref. [2], these authors concluded that cosmic acceleration in the context of  $\Lambda$ CDM could have already peaked and that we might be witnessing a slowing down. This effect was also found previously by ref. [44] using supernova data.

But the process of selecting the most likely correct model also takes into account the number of free parameters. The likelihood of either  $R_h = ct$  or  $\Lambda$ CDM being closer to the “true” model may be determined from the model selection criteria discussed extensively in ref. [23]. A commonly used criterion in cosmology is the Akaike Information Criterion (AIC) [45–47], which prefers models with few parameters to those with many, unless the latter provide a substantially better fit to the data. This avoids the possibility that by using a greater number of parameters, one may simply be fitting the noise.

The AIC is given by  $\text{AIC} = \chi^2 + 2k$ , where  $k$  is the number of free parameters. Among two models  $\mathcal{M}_1$  and  $\mathcal{M}_2$  fitted to the data, the one with the least resulting AIC is assessed as the one more likely to be “true.” If  $\text{AIC}_i$  comes from model  $\mathcal{M}_i$ , the unnormalized confidence that  $\mathcal{M}_i$  is true is the “Akaike weight”  $\exp(-\text{AIC}_i/2)$ . Informally,  $\mathcal{M}_i$  has likelihood

$$\mathcal{L}(\mathcal{M}_i) = \frac{\exp(-\text{AIC}_i/2)}{\exp(-\text{AIC}_1/2) + \exp(-\text{AIC}_2/2)} \quad (6.1)$$

of being closer to the correct model. A lesser known alternative, though based on similar arguments, is the Kullback Information Criterion (KIC), which takes into account the fact that the PDF’s of the various competing models may not be symmetric. The unbiased estimator for the symmetrized version [48] is given by  $\text{KIC} = \chi^2 + 3k$ , very similar to the AIC, but clearly strengthening the dependence on the number of free parameters (from  $2k$  to  $3k$ ). The Bayes

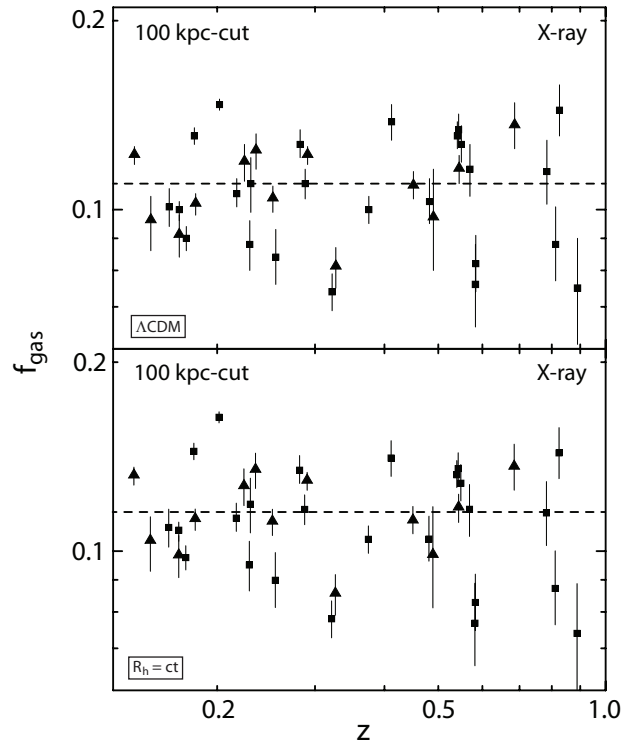


**Figure 3a.** The apparent variation of the X-ray gas mass fraction measured within  $r_{2500}$  as a function of redshift for the 38 clusters in ref. [1], based on *Chandra* X-ray data. Triangles: the cool-core subsample; Squares: the non-cool-core subsample (see text). Both cases assume a single isothermal  $\beta$ -model with the central 100 kpc excised. *Upper panel:* the values are for the reference  $\Lambda$ CDM model ( $\Omega_m = 0.3$ ,  $h \equiv H_0/100 \text{ km s}^{-1} \text{ Mpc}^{-1} = 0.7$ , and  $w_{de} = -1$ ). *Lower panel:* The  $R_h = ct$  Universe. Both results are consistent with the expectation of a constant  $f_{gas}(z)$  (dashed lines) from simulations. The reference  $\Lambda$ CDM fit yields  $f_{gas} = 0.108 \pm 0.020$ , with  $\chi^2_{\text{dof}} = 0.88$  for 36 degrees of freedom (upper panel), and the  $R_h = ct$  fit yields  $f_{gas} = 0.114 \pm 0.021$ , with  $\chi^2_{\text{dof}} = 0.84$  for 38 degrees of freedom (lower panel). By comparison, the cosmic ratio  $\rho_b/(\rho_b + \rho_d)$  measured by *Planck* is  $0.155 \pm 0.006$  [35], and  $0.166 \pm 0.013$  measured by WMAP-9 [39].

Information Criterion (BIC) is perhaps the best known of the three, and represents an asymptotic ( $N \rightarrow \infty$ ) approximation to the outcome of a conventional Bayesian inference procedure for deciding between models [49]. This criterion is defined by  $\text{BIC} = \chi^2 + (\ln N)k$ , and clearly suppresses overfitting very strongly if  $N$  is large.

For the fits discussed in the previous section, these three model selection criteria result in the likelihoods shown in Table 1. The point of listing all three criteria is not so much to dwell on which of these may or may not reflect the importance of free parameters but, rather, to demonstrate that there is general agreement among them—the most commonly used model-selection tools in the literature—that the cluster gas mass fraction data favor the  $R_h = ct$  Universe over  $\Lambda$ CDM. In the case of BIC, considered to be the most reliable among them [45,46], the difference in likelihoods is overwhelming ( $\sim 95\%$  to  $\sim 5\%$ ). This effect is considered to be ‘strong’ when using these criteria. Note also that, in spite of the fact that the Ettori et al. [3] sample uses a different over-density ratio  $\Delta$  than those of refs. [1,2], the likelihood comparisons in Table 1 are all quite similar and consistent with each other. This may be a fortuitous result because simulations have shown that the baryon fraction in clusters can vary depending on the level of concentration towards the core, as a result of several astrophysical effects, including radiative cooling and feedback from winds (see also ref. [50]). It appears that the level of measurement precision we have currently is not

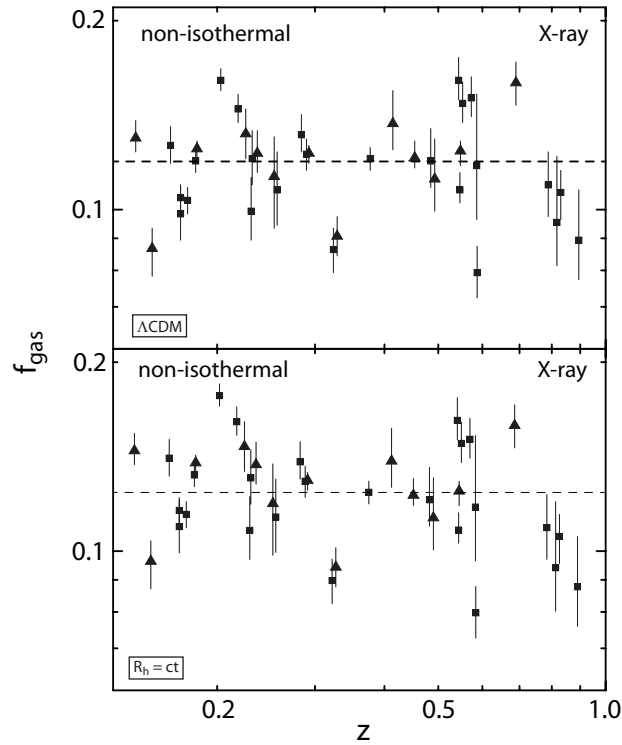


**Figure 3b.** Same as Fig. 3.a, except now assuming a nonisothermal  $\beta$ -model. Triangles and squares have the same meaning. *Upper panel:* the values are for the reference  $\Lambda$ CDM model. *Lower panel:* the  $R_h = ct$  Universe. The fits yield  $f_{\text{gas}} = 0.118 \pm 0.021$ , with  $\chi^2_{\text{dof}} = 0.82$  for 36 degrees of freedom (upper panel), and  $f_{\text{gas}} = 0.124 \pm 0.022$ , with  $\chi^2_{\text{dof}} = 0.86$  for 38 degrees of freedom (lower panel). By comparison, the cosmic ratio  $\rho_b/(\rho_b + \rho_d)$  measured by *Planck* is  $0.155 \pm 0.006$  [35], and  $0.166 \pm 0.013$  measured by WMAP-9 [39].

sufficient to discern between these two values of  $\Delta$ . However, the fact that theory predicts some change in  $f_{\text{gas}}$  with spatial scale suggests that future observations may need to be interpreted more carefully when the baryon fraction is used to do cosmological model comparisons.

Interestingly, these likelihoods are similar to those inferred from our analysis of the cosmic chronometer data [23], and from our consideration of the gamma-ray burst Hubble Diagram [24]. Together, these tests are beginning to paint a consistent picture. At best,  $\Lambda$ CDM may do as well as  $R_h = ct$  in accounting for some of the data, though at a cost—the need to include a larger number of free parameters. But in some cases, such as the cosmic chronometers, the  $\chi^2$  of the  $\Lambda$ CDM fit is inferior to that of  $R_h = ct$ , even though the former has a larger number of unrestricted variables.

Insofar as the use of cluster gas mass fractions to probe the cosmological expansion is concerned, there is considerable room for improvement beyond the current situation. For example, as the precision of the observations continues to improve, and as the hydrodynamic simulations gain in sophistication and complexity, it is becoming more apparent that the adoption of a purely constant fraction  $f_{\text{gas}}$  may be an over-simplification. This ratio apparently changes with radius in any given cluster and, worse, may not be uniformly constant (as evidenced in part by the observed scatter) across a chosen sample (see, e.g., refs [52,53]). At the very minimum, these effects call into question the use of different  $\Delta$ 's to calculate  $f_{\text{gas}}$ . Part of the difficulty is that the best spatially-resolved data are not fully consistent with the assumption of hydrostatic equilibrium, which was used to infer the mass of the X-ray emitting plasma. Recently, substantial progress has been made with cluster observations, driven by weak gravitational lensing, which does not depend on the dynamical state of the cluster [52,53]. Such joint X-ray and weak-lensing

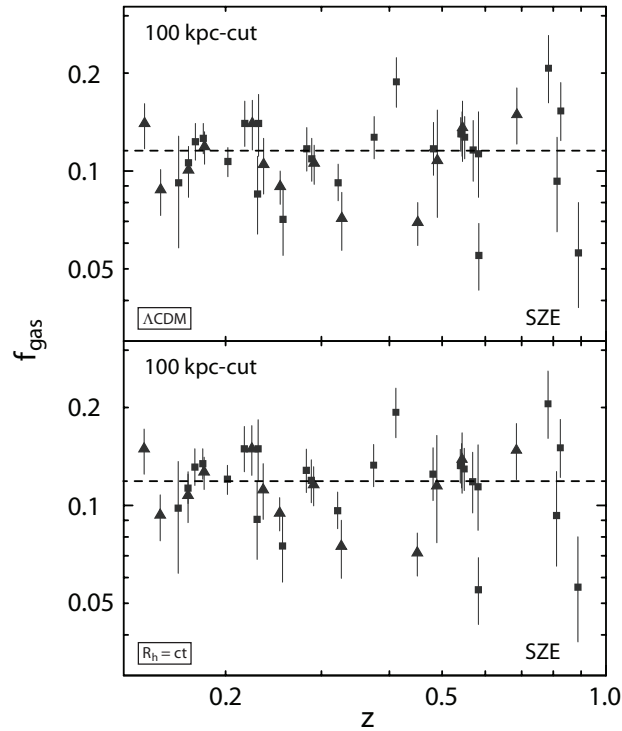


**Figure 3c.** Same as Fig. 3.a, except here for the SZE data. Triangles and squares have the same meaning. The reference  $\Lambda$ CDM fit yields  $f_{\text{gas}} = 0.114 \pm 0.031$ , with  $\chi^2_{\text{dof}} = 0.59$  for 36 degrees of freedom (upper panel), and the  $R_h = ct$  fit yields  $f_{\text{gas}} = 0.117 \pm 0.032$ , with  $\chi^2_{\text{dof}} = 0.57$  for 38 degrees of freedom (lower panel). By comparison, the cosmic ratio  $\rho_b/(\rho_b + \rho_d)$  measured by *Planck* is  $0.155 \pm 0.006$  [35], and  $0.166 \pm 0.013$  measured by WMAP-9 [39].

studies, encompassing the mass distribution out to the virial radius [52] and  $r_{500}$  [53], clearly show a pronounced radial dependence in the value of  $f_{\text{gas}}$  inferred from both weak-lensing and the ratio of hydrostatic equilibrium mass to weak-lensing mass.

Ironically, the best-fit mean gas fractions that we have derived here (for both  $\Lambda$ CDM and  $R_h = ct$ ) are comparable for the two values of  $\Delta$  used in the samples adopted in this paper, in spite of the expected radial dependence in  $f_{\text{gas}}$ . It appears that these two effects, i.e., the radial dependence of  $f_{\text{gas}}$  and the apparent breakdown of hydrostatic equilibrium, largely offset each other, producing an almost constant mass fraction between  $\Delta = 500$  and  $\Delta = 2,500$ . Nonetheless, the model comparison we have carried out here will benefit considerably from the much more detailed and better spatially-resolved measurements that will be made in the near future along the lines reported in refs. [52,53].

In the long run, one would like to match the capabilities of techniques using Type Ia SNe, cluster number counts, weak lensing and BAO to study the possible redshift dependence of  $f_{\text{gas}}$  and its implication for cosmology. But in order to do this, one would need to measure  $f_{\text{gas}}$  to  $\sim 5\%$  accuracy for large samples (i.e.,  $> 500$ ) of hot, massive clusters ( $kT_e > 5$  keV), spanning the redshift range  $0 < z < 2$  [51]. Though the Constellation-X Observatory and *XEUS*, for which these estimates were first developed, are no longer viable future missions, they have evolved into another possible project, known as The Advanced Telescope for High ENergy Astrophysics (ATHENA), which could contribute to the resources necessary to carry out the required observations, if it ever reaches maturity.

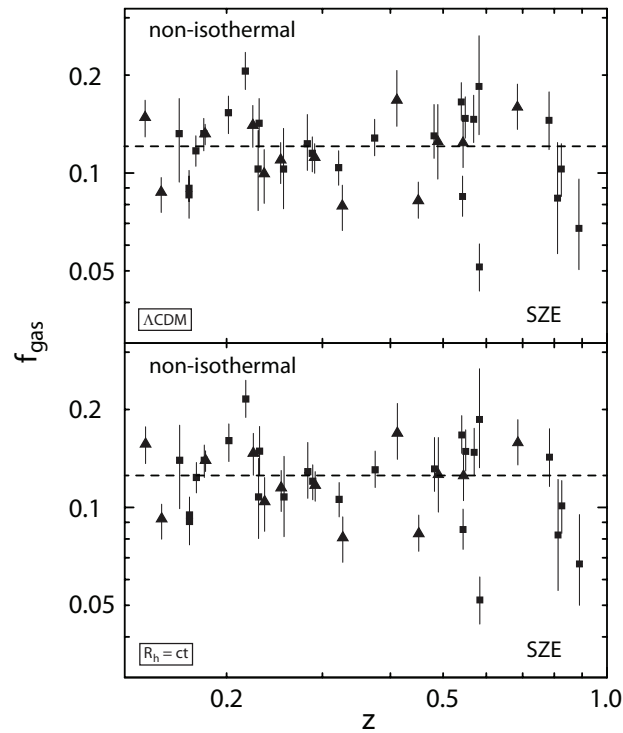


**Figure 3d.** Same as Fig. 3.b, except here for the SZE data. Triangles and squares have the same meaning. The  $\Lambda$ CDM fit yields  $f_{\text{gas}} = 0.120 \pm 0.032$ , with  $\chi^2_{\text{dof}} = 0.67$  for 36 degrees of freedom (upper panel), and  $R_h = ct$  yields  $f_{\text{gas}} = 0.123 \pm 0.033$ , with  $\chi^2_{\text{dof}} = 0.67$  for 38 degrees of freedom (lower panel). By comparison, the cosmic ratio  $\rho_b/(\rho_b + \rho_d)$  measured by *Planck* is  $0.155 \pm 0.006$  [35], and  $0.166 \pm 0.013$  measured by WMAP-9 [39].

## Acknowledgments

I am very grateful to Amherst College for its support through a John Woodruff Simpson Lectureship, and to ISSI in Bern where some of this work was carried out.

**Ethics Statement.** This research poses no ethical considerations.

**Data Accessibility Statement.** All data used in this paper were previously published, as indicated in Table 1.

**Competing Interests Statement.** We have no competing interests.

**Authors' contributions.** FM is the sole author of this paper.

**Funding.** Partial support for this work was provided by the International Space Science Institute in Bern, Switzerland.

## References

1. LaRoque SJ Bonamente M Carlstrom JE Joy MK Nagal D Reese ED and Dawson KS. 2006. X-Ray and Sunyaev-Zel'dovich Effect Measurements of the Gas Mass Fraction in Galaxy Clusters. *ApJ* **652** 917.

Table 1. Likelihood Estimation

Data Source	Criterion	$\Lambda$ CDM	$R_h = ct$
Ref. [3]	AIC	18%	82%
	KIC	8%	92%
	BIC	3%	97%
Ref. [2]	AIC	34%	64%
	KIC	11%	89%
	BIC	6%	94%
Ref. [1] X-ray 100 kpc cut	AIC	13%	87%
	KIC	6%	94%
	BIC	3%	97%
X-ray nonthermal	AIC	66%	34%
	KIC	19%	81%
	BIC	13%	87%
SZE 100 kpc cut	AIC	11%	89%
	KIC	5%	95%
	BIC	3%	97%
SZE nonthermal	AIC	21%	79%
	KIC	9%	91%
	BIC	5%	95%

2. Allen SW Rapetti DA Schmidt RW Ebeling H Morris RG and Fabian AC. 2008. Improved constraints on dark energy from Chandra X-ray observations of the largest relaxed galaxy clusters. *MNRAS* **383** 879.
3. Ettori S Morandi A Tozzi P Balestra I Borgani S Rosati P Lovisari L and Terenziani F. 2009. The cluster gas mass fraction as a cosmological probe: a revised study. *A&A* **501** 61.
4. Eke VR Navarro JF and Frenk CS. 1998. The Evolution of X-Ray Clusters in a Low-Density Universe. *ApJ* **503** 569.
5. Crain RA Eke VR Frenk CS Jenkins AJ McCarthy IG Navarro JF and Pearce ER. 2007. The baryon fraction of  $\Lambda$ CDM haloes. *MNRAS* **377** 41.
6. Sasaki S. 1996. A New Method to Estimate Cosmological Parameters Using the Baryon Fraction of Clusters of Galaxies. *PASJ* **48** L119.
7. Pen U-L. 1997. Measuring the universal deceleration using angular diameter distances to clusters of galaxies. *New Astron* **2** 309.
8. Ettori S Tozzi P and Rosati P. 2003. Constraining the cosmological parameters with the gas mass fraction in local and  $z > 0.7$  galaxy clusters. *A&A* **398** 879.
9. Allen SW Schmidt RW Ebeling H Fabian AC and van Speybroeck L. 2004. Constraints on dark energy from Chandra observations of the largest relaxed galaxy clusters. *MNRAS* **353** 457.
10. White SDM Navarro JF Evrard AE and Frenk CS. 1993. The baryon content of galaxy clusters: a challenge to cosmological orthodoxy. *Nature* **366** 429.
11. Fukugita M Hogan C J and Peebles PJE. 1998. The Cosmic Baryon Budget. *ApJ* **503** 518.
12. Kravtsov AV Daisuke N and Vikhlinin AA. 2005. Effects of Cooling and Star Formation on the Baryon Fractions in Clusters. *ApJ* **625** 588.
13. Ettori S Dolag K Borgani S and Murante G. 2006. The baryon fraction in hydrodynamical simulations of galaxy clusters. *MNRAS* **365** 1021.
14. Planelles S Borgani S Dolag K Ettori S Fabjan D Murante G and Tornatore L. 2013. Baryon census in hydrodynamical simulations of galaxy clusters. *MNRAS* **431** 1487.
15. Melia F. 2007. The cosmic horizon. *MNRAS* **382** 1917.
16. Melia F and Abdelqader M. 2009. The Cosmological Spacetime. *IJMP-D* **18** 1889.
17. Melia F and Shevchuk A. 2012x The  $R_h = ct$  Universe. *MNRAS* **419** 2579.
18. Melia F. 2012. The Cosmic Spacetime. *Australian Physics* **49** 83.
19. Birkhoff G. 1923. *Relativity and Modern Physics*. Harvard University Press, Cambridge.
20. Weyl H. 1923. Zur Allgemeinen Relativitätstheorie. *Z Phys* **24** 230.
21. Misner CW and Sharp DH. 1964. Relativistic Equations for Adiabatic, Spherically Symmetric Gravitational Collapse. *Phys. Rev.* **136** 571.

22. Milne EA. 1933. World-Structure and the Expansion of the Universe. Mit 6 Abbildungen. *Zeitschrift für Astrophysik* **6** 1.
23. Melia F and Maier RS. 2013. Cosmic Chronometers in the  $R_h = ct$  Universe. *MNRAS* **432** 2669.
24. Wei J-J Wu X and Melia F. 2013. The Gamma-ray Burst Hubble Diagram and its Implications for Cosmology. *ApJ* **772** 43.
25. Melia F. 2013. High- $z$  Quasars in the  $R_h = ct$  Universe. *Astrophys. J.* **764** 72.
26. Melia F. 2014. Angular Correlation of the CMB in the  $R_h = ct$  Universe. *A&A* **561** 80.
27. Melia F. 2014. The Premature Formation of High Redshift Galaxies. *AJ* **147** 120.
28. Sarazin CL. 1988. X-Ray Emission from Clusters of Galaxies, Cambridge University Press: Cambridge.
29. Cavaliere A and Fusco-Fermiano R. 1976. X-rays from hot plasma in clusters of galaxies. *A&A* **49** 137.
30. Vikhlinin A Kravtsov A Forman W et al. 2006. Chandra Sample of Nearby Relaxed Galaxy Clusters: Mass, Gas Fraction, and Mass-Temperature Relation. *ApJ* **640** 691.
31. Allen SW Evrard AE and Mantz AB. 2011. Cosmological Parameters from Observations of Galaxy Clusters. *A&A* **49** 409.
32. Riess AG Filippenko AV Challis P et al. 1998. Observational Evidence from Supernovae for an Accelerating Universe and a Cosmological Constant. *Astron. J.* **116** 1009.
33. Perlmutter S Aldering G Goldhaber G et al. 1999. Measurements of Omega and Lambda from 42 High-Redshift Supernovae. *Astrophys. J.* **517** 565.
34. Delubac T. et al. 2015. Baryon acoustic oscillations in the Lyalpha forest of BOSS DR11 quasars. *Astron. Astrophys.* **574** A59.
35. Ade PAR et al. 2013. Planck 2013 results. XVI. Cosmological parameters. *Astron. Astrophys.* **571** A16.
36. Bennett CL et al. 2003. First-Year Wilkinson Microwave Anisotropy Probe (WMAP) Observations: Foreground Emission. *Astrophys. J. Sup.* **148** 97.
37. Copi CJ Huterer D Schwarz DJ and Starkman GD. 2009. *MNRAS* **399** 295.
38. Copi CJ Huterer D Schwarz D and Starkman GD. 2013. No large-angle correlations on the non-Galactic microwave sky. *MNRAS* in press (arXiv:1310.3831).
39. Bennett CL et al. 2013. Nine-year Wilkinson Microwave Anisotropy Probe (WMAP) Observations: Final Maps and Results. *ApJS* **208** 20.
40. Watson DF Berlind AA and Zentner AR. 2011. A Cosmic Coincidence: The Power-law Galaxy Correlation Function. *ApJ* **738** article id. 22.
41. Melia F and Fatuzzo M. 2016. The Epoch of Reionization in the  $R_h = ct$  Universe. *MNRAS* **456** 3422.
42. Lewis GF. 2013. Matter matters: unphysical properties of the  $R_h = ct$  universe. *MNRAS* **432** 2324.
43. Cárdenas VH Bernal C and Bonilla A. 2013. Cosmic slowing down of acceleration using  $f_{\text{gas}}$ . *MNRAS* **433** 3534.
44. Shafieloo A Sahni V and Starobinsky AA. 2010. Invisible Universe: Proceedings of the Conference. AIP Conference Proceedings **1241** 294.
45. Liddle AR. 2004. How many cosmological parameters? *MNRAS* **351** L49.
46. Liddle AR. 2007. Information criteria for astrophysical model selection. *MNRAS* **377** L74.
47. Tan MYJ and Biswas R. 2012. The reliability of the Akaike information criterion method in cosmological model selection. *MNRAS* **419** 3292.
48. Cavanaugh JE. 1999. A large-sample model selection criterion based on Kullback's symmetric divergence. *Statist. Probab. Lett.* **42** 333.
49. Schwarz G. 1978. Estimating the dimension of a model. *Ann. Statist.* **6** 461.
50. Velliscig M van Daalen MP Schaye J McCarthy IG Cacciato M Le Brun AMC and Dalla VC. 2014. The impact of galaxy formation on the total mass, mass profile and abundance of haloes. *MNRAS* **442** 2641.
51. Rapetti D Allen SW Mantz A. 2008. The prospects for constraining dark energy with future X-ray cluster gas mass fraction measurements. *MNRAS* **388** 1265.
52. Okabe N et al. 2014. Universal profiles of the intracluster medium from Suzaku X-ray and Subaru weak-lensing observations. *PASJ* **66** 99.
53. Donahue M et al. 2014. CLASH-X: A Comparison of Lensing and X-ray Techniques for Measuring the Mass Profiles of Galaxy Clusters. *ApJ* **794** 136.